

End compression of sandwich columns

N.A. Fleck*, I. Sridhar

Department of Engineering, University of Cambridge, Trumpington Street, Cambridge CB2 1PZ, UK

Received 29 November 2000; revised 16 July 2001; accepted 18 July 2001

Abstract

Sandwich columns, comprising woven glass fibre reinforced epoxy face sheets and PVC polymer foam cores, have been tested under edgewise compressive loading. Failure is by Euler macrobuckling, shear macrobuckling or by face sheet microbuckling, depending upon the material combination and geometry of column. Simple analytical models are developed for the axial strength, and these are in good agreement with the experimental values for each failure mode. Collapse mechanism maps are constructed to illustrate the dependence of failure mode upon the geometry and relative density of the core; and minimum weight designs are determined as a function of the appropriate structural load index. © 2002 Elsevier Science Ltd. All rights reserved.

Keywords: B. Mechanical properties; B. Buckling; Sandwich structures

1. Introduction

Sandwich panels, consisting of two stiff, strong face sheets and a light weight core, can be designed to possess a high bending stiffness and strength at low weight; consequently, they are used increasingly in land, sea and air vehicles. To a good approximation, the face sheets carry the bending and in-plane loads, whilst the core carries transverse shear. Commonly used materials for sandwich panels are metallic or composite face sheets, with a foam core made from a polymeric or metallic foam, or wood. The fundamentals of sandwich panel construction and design methods are given by Allen [1] and Zenkert [2]; recent surveys on the use of foam cores are provided by Gibson and Ashby [4] and by Ashby et al. [5].

An important loading configuration for sandwich panels is end compression: this is the subject of the current article. Failure under end compression is by a number of competing mechanisms including face sheet microbuckling or yielding, face sheet wrinkling, macroscopic shear buckling and Euler buckling [6,7]. In contrast, when a sandwich panel is subjected to 3-point or 4-point bend loading, failure may occur by face sheet yield, fracture of the core in shear, face sheet wrinkling or indentation beneath the rollers [8–11].

In this study, sandwich columns have been manufactured with a core of Divinycell closed-cell PVC foam and face

sheets comprising woven glass fibre — epoxy. The columns are subjected to end compression and the strength and operative failure mode are determined as a function of the length of the column and the relative density $\bar{\rho}$ of the core. The objectives are to identify the operative failure modes, and to develop simple analytical models of the compressive strength. Failure mode maps are constructed to show the dominant failure mode as a function of geometry and relative density of core, and minimum weight designs are determined as a function of a structural load index. We begin by giving analytical expressions for the uniaxial compressive strength for the anticipated competing failure modes.

2. Analytical formulae for competing failure modes of sandwich struts

Consider a sandwich column of length l , with ends constrained against rotation, and subjected to an end load P , as sketched in Fig. 1. In this study, we specialise to the case where the sandwich column comprises composite face sheets and a polymeric foam core. Consequently, the face sheets are treated as a linear elastic solid with a compressive strength σ_{cr} due to fibre microbuckling. The core also behaves in a linear elastic manner since the yield strain for polymeric foams is of the order of several percent compared with a failure strain of the face sheets of about 1% in tension and compression. At least four possible failure modes exist for such sandwich columns: Euler

* Corresponding author. Tel.: +44-1223-332-650;
fax: +44-1223-332-662.

E-mail address: naf1@eng.cam.ac.uk (N.A. Fleck).

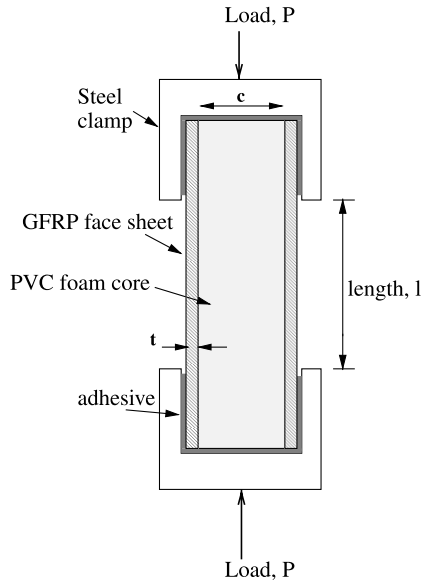


Fig. 1. A sandwich column subjected to end compression.

macro buckling, elastic core shear macro buckling, plastic micro buckling of the face sheets and face wrinkling. These failure modes are sketched in Fig. 2.

2.1. Elastic buckling in bending and in shear

Two modes of elastic buckling are possible: an Euler buckling mode involving bending of the sandwich column and a core shear mode. For the case of a strut with built-in ends (which are constrained against rotation), the Euler buckling load P_E is:

$$P_E = \frac{4\pi^2(EI)_{eq}}{l^2} \quad (1)$$

in terms of the equivalent flexural rigidity $(EI)_{eq}$, as given by:

$$(EI)_{eq} = \frac{btd^2E_f}{2} + \frac{bt^3E_f}{6} + \frac{bc^3E_c}{12} \approx \frac{btc^2E_f}{2} \quad (2)$$

Here, E_f and E_c are the Young's moduli for the face sheet and core materials, respectively, b is the width of the sandwich column, t is the face sheet thickness and c is the core

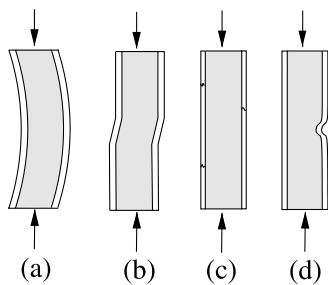


Fig. 2. Failure modes in sandwich columns subjected to edge compression. (a) Euler macro buckling; (b) core shear macro buckling; (c) face sheet micro buckling and (d) face sheet wrinkling.

thickness, see Fig. 1. The dimension $d \equiv t + c$ is the spacing between the mid-planes of the face sheets.

The core shear buckling load P_s is set by the shear stiffness of the core, viz,

$$P_s = (AG)_{eq} \quad (3)$$

where the equivalent shear rigidity $(AG)_{eq}$ of the core is:

$$(AG)_{eq} \approx bcG_c \quad (4)$$

in terms of the shear modulus of the core G_c and the cross-sectional area bc of the core [2]. We note in passing that Euler buckling occurs at a lower load than shear buckling, for sufficiently slender columns.

In the present study, it is instructive to treat Euler and shear buckling as two independent modes. However, these buckling modes can interact at transition values of strut slenderness ratio [2] to give a combined collapse load P_{cr} , where:

$$\frac{1}{P_{cr}} = \frac{1}{P_E} + \frac{1}{P_s} \quad (5)$$

2.2. Plastic micro buckling of the face sheets

Plastic micro buckling of the face sheets occurs when the axial compressive stress within the face sheets attains the plastic micro buckling strength σ_{cr} . Since the elastic core is taken to be much more compliant than that of the face sheets, the overall collapse load is:

$$P_f = 2tb\sigma_{cr} \quad (6)$$

It is now well established that the micro buckling strength σ_{cr} of the composite face sheet depends upon the degree of fibre misalignment and upon the shear strength of the matrix, see for example the review of Fleck [12]. In the present study, we have measured σ_{cr} independently and treat it as a material property, rather than rely upon the predictions of particular micromechanical models.

2.3. Face wrinkling

Wrinkling is the short-wavelength elastic buckling of the face sheets. Upon assuming that the face sheets buckle as elastic beams upon a linear elastic foundation, the compressive bifurcation stress in the face sheet for wrinkling is given conservatively by [2,3]:

$$\sigma_{fw} = 0.5(E_fE_cG_c)^{1/3} \quad (7)$$

3. Experimental method

3.1. Test materials

The sandwich columns comprised face sheets made from woven glass fibres and a PVC foam core, as follows. The face sheets were made from 4 layers of eight harness satin

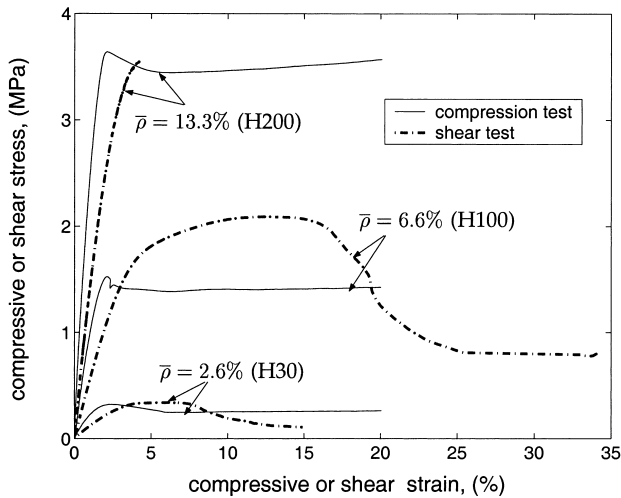


Fig. 3. Nominal stress versus nominal strain response of the PVC foams in compression and in shear.

weave 7781 E-glass fibres. Each layer of cloth was pre-impregnated with 914G epoxy resin (trade name Hexcel Fibredux), giving a volume fraction of about 63% glass fibres and an average density ρ_f of 1.77 mg m^{-3} .

The sandwich cores were made from closed-cell PVC foam (trade name *Divinycell*¹) of thickness 10 mm. Three densities of foam, H30, H100 and H200 were used; these have an absolute density ρ_c of 37, 93 and 186 Mg m^{-3} , and a relative density of 2.6, 6.6 and 13.3%, respectively. The composite face sheets were adhered to the PVC foam using two-component, liquid polyurethane adhesive (XB5090-1/XB5304²) and cured at room temperature.

3.1.1. Baseline properties of face sheet and core

Uniaxial compression tests were conducted on the face sheet material by performing Celanese tests on coupons of width 10 mm, thickness 1 mm and gauge length 8 mm, at a nominal strain rate of 10^{-3} s^{-1} . The measured axial Young’s modulus was 30 GPa, and the compressive microbuckling strength σ_{cr} of the face sheets was 350 MPa, at a failure strain of 1.2% [13].

Compression and shear tests were performed on the PVC closed-cell foams at a strain rate of 10^{-3} s^{-1} , as follows. Uniaxial compression tests were conducted on 50 mm cubes, parallel to the rise direction. Shear tests on the H30 and H100 PVC foam were performed on $100 \text{ mm} \times 25 \text{ mm} \times 10 \text{ mm}$ rectangular blocks using a double lap shear configuration. Attempts to conduct a satisfactory

double-lap shear test on the H200 foam failed however: interfacial failure always occurred between the foam and a loading plate. To overcome this problem, Deshpande and Fleck [14] performed shear tests on the H200 foam using an Arcan test rig. The uniaxial and shear stress–strain curves for each of the foams are plotted in Fig. 3, and the values of the axial and shear moduli are summarised in Table 1 [13].

Gibson and Ashby [4] have shown that the shear modulus G_c of a foam core scales with its relative density $\bar{\rho}$ and the cell wall shear modulus G_s according to:

$$\frac{G_c}{G_s} = \alpha \bar{\rho}^m \tag{8}$$

where α and m are treated as material constants.

Here, we assume $\alpha = 1$ and curve fit Eq. (8) to our measured values G_c , giving $G_s = 2.58 \text{ GPa}$ and $m = 1.5$. Similarly, the Young’s modulus of the foam core E_c scales with $\bar{\rho}$ according to:

$$\frac{E_c}{E_s} = \beta \bar{\rho}^n \tag{9}$$

and a curve fit to our measured values of E_c gives $n = 1.5$, and $E_s = 6.0 \text{ GPa}$, with $\beta = 1$. The data for G_c and E_c measured in the present study, and reported in Table 1, are in reasonable agreement with the handbook values [15].

3.2. Test method

End-compression tests were performed on the sandwich columns in accordance with the ASTM standard C364-61 [16]. Specimens were cut from larger panels using a circular diamond saw, and were of gauge length l in the range 19–440 mm and width b in the range 15–36 mm. In order to prevent end brooming, the specimens were bonded into U-shaped steel clamps with epoxy adhesive, providing a built-in loading condition, as sketched in Fig. 1. Strain gauges were used to measure the longitudinal strain at mid-length of the front and back faces of the sandwich panels. Similarly, the shear strain within the core was measured using a $0/45/90^\circ$ strain gauge rosette at mid-thickness and at mid-length. The specimens were compressed axially at a constant cross-head displacement rate of $10^{-3} \text{ mm s}^{-1}$, until failure occurred. The applied load was measured using the load cell of the screw-driven test machine, and the cross-head displacement was recorded by a linear voltage displacement transducer (LVDT). Care was taken to ensure that the sandwich columns were flat and parallel: the maximum angle of misalignment of either face was 0.3° .

Table 1
Measured mechanical properties of the PVC polymer foam cores

Foam and relative density, $\bar{\rho}$	Cell size (μm)	Young’s modulus E_c (MPa)	Shear modulus G_c (MPa)
H30 (2.6%)	800	26	13.0
H100 (6.6%)	400	105	43.8
H200 (13.3%)	200	293	110

Table 2

Summary of end compression tests on sandwich columns. All specimens have a face sheet thickness $t = 1.0$ mm and a core thickness $c = 10.0$ mm. CS = Core shear macrobuckling, E = Euler macrobuckling, M = microbuckling

$\bar{\rho}$ (%)	Length l (mm)	Width b (mm)	Gross-section strength, (MPa)	Axial strain at peak load (%)	Observed collapse mode
2.6	20.3	36.0	21.1	0.80	CS
	47.8	34.7	17.0	0.45	CS
	49.4	35.5	13.8	0.20	CS
	78.9	28.1	13.8	0.24	CS
6.6	19.2	34.0	42.7	0.75	CS
	41.9	33.7	37.1	0.72	CS
	48.9	33.5	40.0	0.68	CS
	54.3	34.5	39.8	0.78	CS
	67.8	36.1	37.8	0.65	CS
	386	15.0	27.6	0.44	E
13.3	21.2	34.9	65.0	0.95	M
	41.1	36.3	59.1	0.90	M
	47.5	35.3	51.6	0.95	M
	306	20.0	31.0	0.40	E
	439	20.0	23.5	0.35	E

4. Results

We report on the compression response of the sandwich columns and compare the analytical formulae presented in Section 2 with the measured failure stresses. A summary of the geometries employed in the sandwich column tests is given in Table 2, together with the observed failure modes of shear macrobuckling, Euler buckling and face sheet microbuckling. The axial load versus end shortening response was almost linear up to peak load: the table includes the peak nominal stress based on the full cross-section $(c + 2t)b$, and the associated axial failure strains are measured from the strain gauges mounted on the face sheets.

The observed gross-section stress at failure is plotted

against the strut length in Fig. 4, for each density of core. Additionally, the predicted failure strength is shown for core shear, Euler buckling and microbuckling. The predictions support the observed strengths, as follows. At short strut lengths ($l < 300$ mm), the microbuckling strength of the sandwich column with a H200 core is less than the core shear buckling strength, and so these columns fail by microbuckling. At larger strut lengths, Euler buckling dominates; interaction between face microbuckling and Euler macrobuckling leads to observed strengths somewhat below the predicted values for Euler macrobuckling.

In contrast, the foams of lower density (H100 and H30) have sufficiently low shear moduli for them to fail by core shear at short strut lengths. Again, struts of length exceeding

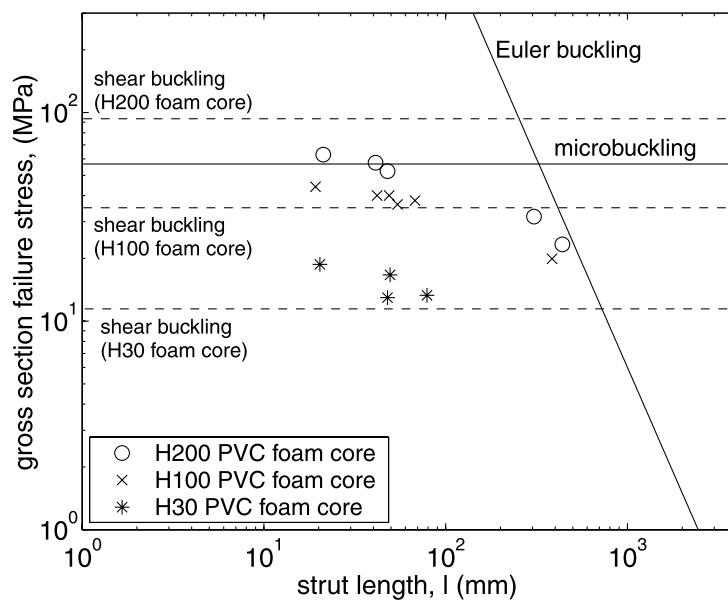


Fig. 4. Comparison of measured failure stress with analytical predictions for end compressed sandwich struts. The dotted lines represent Eq. (3), and denote shear buckling for the three densities of PVC foams.

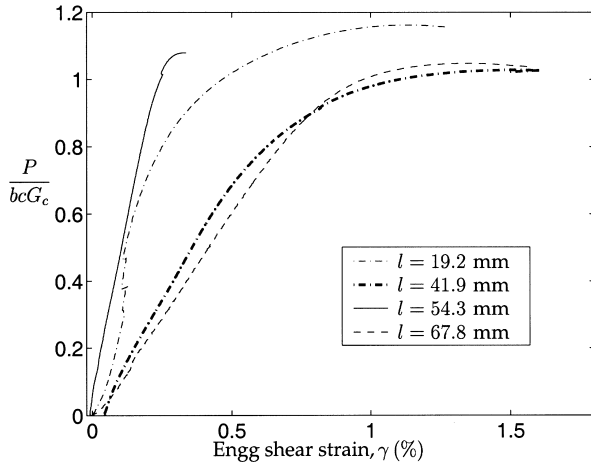


Fig. 5. Measured core shear strain versus normalised load for end compressed sandwich columns comprising a H100 PVC foam core.

about 300 mm undergo Euler buckling. The largest discrepancy of prediction versus measurement is for the short struts with the H30 core. These struts have a length $l = 20$ mm, comparable to the core thickness $c = 10$ mm, and for such struts, the assumption of uniform axial and shear straining within the core breaks down, and the formula (3) becomes inaccurate.

Support for the observed failure modes is as follows. Euler buckling was identified by the overall deformation mode of the strut. Core shear gave a characteristic buckling mode as shown in Fig. 2(b). Also, strain gauge rosettes attached to the side face of the sandwich core revealed the accumulation of shear strain at an axial load level of approximately that given by Eq. (3), see Fig. 5 for the case of a H100 foam core. The presence of small imperfec-

tions in column straightness led to the progressive build-up of shear strain in the core with increasing load, followed by a dramatic increase in shear strain as the core shear buckling load P_s is approached. Similar results were obtained for core shear of the H30 core (not shown). Microbuckling of the composite face sheets is a catastrophic event and occurred at an axial strain of about 1% in both the Celanese tests on the face sheets, and in the sandwich column tests. Examination of the fracture surfaces in the scanning electron microscope confirmed that this failure mode was activated for the short columns with a H200 core.

4.1. Collapse mechanism map

A collapse mechanism map is constructed in Fig. 6, showing the observed and predicted collapse mode as a function of the non-dimensional geometric parameter l/c and the relative density $\bar{\rho}$, $t/c = 0.1$. The boundaries of each collapse regime were obtained by equating the predicted collapse loads for each mode in turn. Contours of structural load index $\bar{P} \equiv P/(lb\sigma_{cr})$ have been added, based upon relations (1), (3) and (6). Excellent agreement is noted between the predicted and observed collapse modes, as already noted above. The highest collapse loads are predicted for short columns with a high-density core.

Similar maps have been devised by Gibson and Ashby [4] for sandwich beams in 3-point bending with polymeric foam cores and metallic face sheets, and by Steeves and Fleck [13] for sandwich beams with composite face sheets and PVC foam core. These maps are useful in the development of minimum weight designs as a function of structural load index, as discussed below.

4.2. Minimum weight design for a given axial strength

Typically, in the optimal design of a sandwich column, it is required to select the density of foam core and column geometry which minimises the overall mass for a given load carrying capacity. For the case of a sandwich column subjected to axial compression, the appropriate structural load index is $\bar{P} \equiv P/(lb\sigma_{cr})$, and the non-dimensional mass of the column \bar{M} is defined by

$$\bar{M} \equiv \frac{M}{bl^2\rho_f} = 2\frac{t}{l} + \frac{c}{l}\frac{\rho_c}{\rho_f} \tag{10}$$

The dependence of geometry and foam density upon structural load index is determined by considering each collapse mode in turn. For face sheet microbuckling, relation (6) gives:

$$\bar{P} \equiv \frac{P}{lb\sigma_{cr}} = 2\frac{t}{l} \tag{11}$$

while for overall elastic macrobuckling, relations (1), (3) and (5) provide:

$$(\bar{P})^{-1} = \frac{1}{2\pi^2} \frac{\sigma_{cr}}{E_f} \left(\frac{l}{c}\right)^2 \frac{l}{t} + \frac{\sigma_{cr}}{G_c} \frac{l}{c} \tag{12}$$

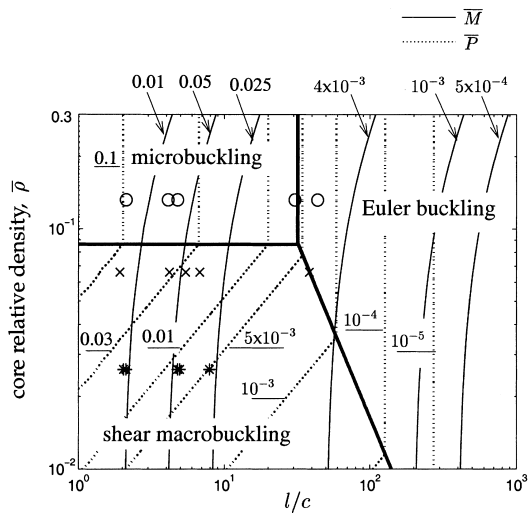


Fig. 6. Failure mode map of sandwich column comprising woven glass fibre composite face sheets and PVC polymer foam core subjected to end compression. Experimental data are included. The ratio of core thickness to face sheet thickness l/c is fixed at 10. O: sandwich columns with $\bar{\rho} = 13.3\%$ and x: sandwich columns with $\bar{\rho} = 6.6\%$ and \star : sandwich columns with $\bar{\rho} = 2.6\%$.

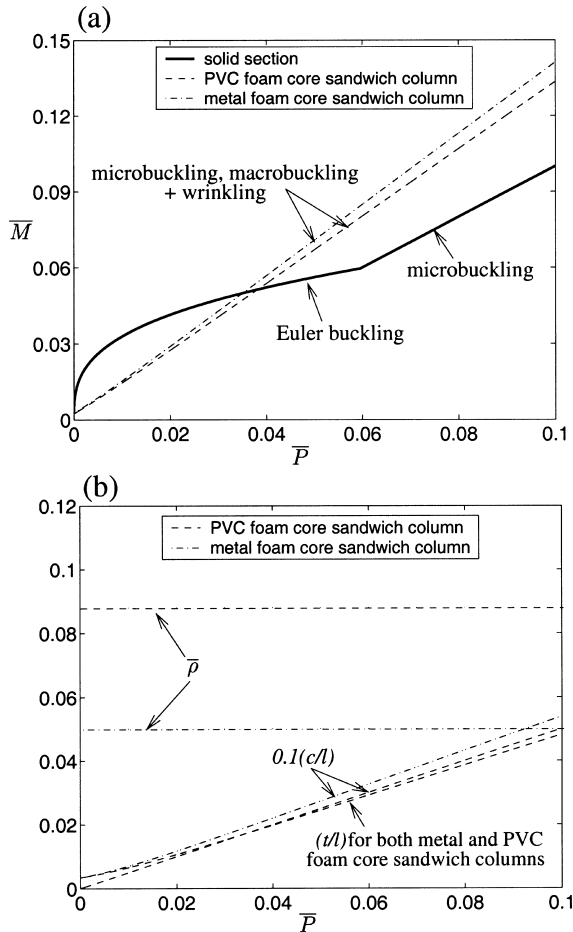


Fig. 7. (a) Variation of mass index with load index for solid section, PVC core sandwich column ($m = 1.5$, $n = 1.5$, $E_f/\sigma_{cr} = 85.7$, $(\alpha G_s)/\sigma_{cr} = 7.37$ and $\rho_f/\rho_s = 1.26$) and metal foam core sandwich column ($m = n = 2$, $E_f/\sigma_{cr} = 85.7$, $(\alpha G_s)/\sigma_{cr} = 74$ and $\rho_f/\rho_s = 0.66$). (b) Optimal values of relative density, c/l and t/l versus \bar{P} .

and for face sheet wrinkling, Eq. (7) gives:

$$\bar{P} = \frac{t}{l} \frac{(E_f E_c G_c)^{1/3}}{\sigma_{cr}} \quad (13)$$

The minimum weight design is found by calculating the minimum mass \bar{M} necessary to suppress all possible collapse mechanisms for a given value of load index \bar{P} . Thus, the dominant mode, or combination of modes, is the one with the largest value of \bar{M} at each value of \bar{P} . We find that collapse is always by a combination of microbuckling, wrinkling and macrobuckling; the associated values of $\bar{\rho}$, t/l and c/l are given as follows.

The optimal core density follows from Eqs. (8), (9), (11) and (13), and is expressed by:

$$\bar{\rho} = \left(\frac{8\sigma_{cr}^3}{\alpha\beta E_f E_s G_s} \right)^{1/m+n} \quad (14)$$

The normalised face sheet thickness t/l is related directly to \bar{P} by Eq. (11), and the normalised core thickness c/l is

obtained by equating the microbuckling load Eq. (11) to the macrobuckling load Eq. (12), to give:

$$\frac{l}{c} = -\frac{\pi^2}{2} \frac{E_f}{\sigma_{cr}} \frac{\sigma_{cr}}{G_c} \bar{P} + \left[\left(\frac{\pi^2}{2} \frac{E_f}{\sigma_{cr}} \frac{\sigma_{cr}}{G_c} \bar{P} \right)^2 + \pi^2 \frac{E_f}{\sigma_{cr}} \right]^{1/2} \quad (15)$$

with the foam core shear modulus G_c specified by Eqs. (8) and (14). The mass index \bar{M} is obtained as a function of \bar{P} via Eqs. (10), (14) and (15).

The minimum mass of column \bar{M} is plotted as a function of \bar{P} in Fig. 7(a). For realistic values of \bar{P} , collapse is by combined microbuckling, wrinkling and macrobuckling. The optimal values of $\bar{\rho}$, c/l and t/l are given in Fig. 7(b): we find that $\bar{\rho}$ equals 0.090, independent of \bar{P} , while c/l increases from 0.03 to 0.5 and t/l increases from almost zero to 0.05 as \bar{P} increases from zero to the upper practical limit of 0.1.

4.2.1. Comparison of the performance of a sandwich column containing a polymer foam core with that of other columns

It is instructive to compare the minimum weight designs for sandwich columns comprising a PVC core with the equivalent columns comprising a metallic foam core; the comparison is included in Fig. 7(a). For definiteness, we shall assume that the face sheets comprise the same glass fibre composite as that used in the above experimental study. The mechanical properties of the metal foam are taken to be representative of current commercially available closed cell aluminium alloy foams, as reviewed by Ashby et al. [5]. The shear modulus G_c scales with relative density according to relation (8), with $\alpha = 1$, $m = 2$; the shear modulus of the cell walls is taken to be that of aluminium–silicon casting alloys, $G_s = 26$ GPa, and the density of the cell walls is $\rho_s = 2.7$ Mg m⁻³. The Young's modulus E_c is given by Eq. (9), with $\beta = 1$, $n = 2$ and $E_s = 70$ GPa. A calculation of the minimum mass \bar{M} for the sandwich column gives similar predictions to those obtained for the PVC foam core: collapse is by combined microbuckling, wrinkling and macrobuckling for realistic values of \bar{P} , see Fig. 7(a). The optimal relative density of the metallic foam core is about 0.05 over the practical range of \bar{P} , with the geometrical parameters c/l and t/l taking on similar values to those given for the PVC foam cores, as summarised in Fig. 7(b). The sandwich column with a PVC foam core is about 4% lighter than that for a column of the same load carrying capacity, but with a metallic foam core.

Now consider the case of a solid composite column of rectangular cross-section, subjected to end compression. Such a column will collapse by some combination of microbuckling and Euler macrobuckling: the transverse shear modulus is assumed to be sufficiently large that shear macrobuckling can be neglected. Since no foam core is present, wrinkling can also be ignored. At low values of \bar{P} (< 0.06), the minimum weight design collapses by Euler

macro buckling, and relation (1) can be re-expressed to give:

$$\bar{M} = \left[\frac{3}{\pi^2} \frac{\sigma_{cr}}{E_f} \bar{P} \right]^{1/3} \quad (16)$$

However, for $\bar{P} > 0.06$, micro buckling dominates, and the minimum weight is achieved at zero core thickness, with:

$$\bar{M} = 2 \frac{t}{l} = \bar{P} \quad (17)$$

by Eqs. (10) and (11). We conclude from Fig. 7(a) that the solid column has a lower weight than either sandwich column for an axial strength \bar{P} exceeding 0.034, and for lightly loaded columns with $\bar{P} < 1.4 \times 10^{-6}$. In the intermediate but practical regime of \bar{P} values, the sandwich columns are significantly lighter than the solid column.

5. Concluding remarks

Edge compression tests have been performed on sandwich columns consisting of closed-cell PVC foam cores and glass fibre reinforced epoxy face sheets. A number of competing failure modes are observed: shear macro buckling, Euler macro buckling and face sheet micro buckling. Face sheet wrinkling was not observed as the wrinkling strength exceeded either the micro buckling strength or the macro buckling strength, depending upon the relative density of core and slenderness of column. The predicted failure loads for competing failure modes agree reasonably well with the observed strengths. Collapse mechanism maps, with axes of normalised column length (l/c) and core relative density, are useful for displaying the dominant failure modes.

The minimum weight design of sandwich columns has been carried out for all possible combinations of collapse mode, for sandwich columns comprising a PVC or aluminium foam core, and for composite columns of solid section. The optimal choice of column construction depends upon the required structural load index \bar{P} required of the column. It remains to explore the effect of choice of face sheet, and loading configuration such as 3-point bending in order to determine whether the above conclusions will require modification in the more general case.

Acknowledgements

The authors are grateful for financial support from ONR (USA), under contract No. N00014-91-J-1916, and wish to thank Mr John Ellis of Hexcel Composite Materials, Duxford, UK for providing the glass fibre prepregs and manufacturing facilities.

References

- [1] Allen HG. Analysis and design of structural sandwich panels. Oxford: Pergamon Press, 1969.
- [2] Zenkert D. An introduction to sandwich construction. London: Engineering Materials Advisory Services, 1995.
- [3] Hoff NJ, Mautner SE. Buckling of sandwich type panels. *J Aeronaut Sci* 1945;12:285–97.
- [4] Gibson LJ, Ashby MF. Cellular solids: structure and properties. 2nd ed. Cambridge: Cambridge University Press, 1997.
- [5] Ashby MF, Evans A, Fleck NA, Gibson LJ, Hutchinson JW, Wadley HNG. Metal foams: a design guide. Heinemann, USA: Butterworth, 2000.
- [6] Ackers P. The efficiency of sandwich struts utilising a calcium Alginate core Rep Memo, 2015 (UK Aeronautical Research Council, Farnborough, Hants, UK), 1945.
- [7] Wittrick WH. A theoretical analysis of the efficiency of sandwich construction under compressive end load. Rep Memo, 2016 (UK Aeronautical Research Council, Farnborough, Hants, UK), 1945.
- [8] Triantafillou TC, Gibson LJ. Failure mode maps for foam core sandwich beams. *Mater Sci Engng* 1989;85:37–53.
- [9] Triantafillou TC, Gibson LJ. Minimum weight design of foam core sandwich panels for a given strength. *Mater Sci Engng* 1987;85:55–62.
- [10] Chen C, Harte A-M, Fleck NA. The plastic collapse of sandwich beams with a metallic foam core. *Int J Mech Sci* 2001;43:1483–506.
- [11] McCormack TM, Miller R, Kesler O, Gibson LJ. Failure of sandwich beams with metallic foam cores. *Int J Solid Struct* 2001;38:4901–20.
- [12] Fleck NA. Compressive failure of fibre composites. *Adv Appl Mech* 1997;33:43–117.
- [13] Steeves C, Fleck NA. Failure modes in sandwich beams with composite face-sheets and PVC foam cores. ASTM Conference on Composite Structure, Florida, 2000.
- [14] Deshpande VS, Fleck NA. Multi-axial yield behaviour of polymer foams. *Acta Mater* 2001;49:1859–66.
- [15] Divinycell technical manual: H grade, high performance core materials for sandwich construction, Divinycell International Limited, Gloucester-GL4 7SJ, 1985.
- [16] ASTM C364-61. Standard test method for edgewise compressive strength of flat sandwich constructions, vol. 15.03. American Society of Testing and Materials, 1989 p. 13–5.